Peroxyoxalate Chemiluminescence Detection for Capillary Electrophoresis Using Membrane Collection

Loranelle L. Shultz,* Scott Shippy,** Timothy A. Nieman,† Jonathan V. Sweedler
University of Illinois at Urbana-Champaign, Urbana, IL 61801, USA

Received 27 May 1997; accepted 30 October 1997

Abstract: Capillary electrophoresis (CE) is often limited by the need to measure nanoliter-volume, low-concentration analytes with selectivity and specificity. A post-column chemiluminescence (CL) method is described in which the capillary effluent is collected on a membrane which has been coated with a peroxyoxalate CL reagent, bis(2,4,6-trichlorophenyl)oxalate. After the CE run, the CL reaction is initiated on the membrane by applying hydrogen peroxide, a scientific charge-coupled device (CCD) camera images the resultant CL emission, and an electropherogram is reconstructed. This postcolumn detection scheme decouples the separation parameters from detection and allows longer lived CL reagents to be used with fast separations. As the reaction is catalyzed by imidazole, CL intensities and lifetimes resulting from imidazole- and non-imidazole-running buffers are compared. The postcolumn CL method is compared to on-line UV absorbance detection for a mixture of dansylated amino acids, with limits of detection (LODs) of 1.5 μM (13 fmol) and separation efficiencies of 170,000 plates. The ability to preserve the sample on the membrane allows several selective detection schemes to be employed; the combination of postcolumn chemiluminescence and radionuclide detection from a single electrophoretic separation is demonstrated. J Micro Sep 10: 329–337, 1998

Key words: *capillary electrophoresis; postcolumn detection; membrane collection; peroxyoxalate chemiluminescence; radionuclide detection*

INTRODUCTION

Capillary electrophoresis (CE) is currently one of the highest efficiency and lowest volume separation techniques available to the analytical chemist [1–3]. Due to the low sample volumes required for CE and the trace analyte amounts present in bioanalytical and biomedical applications, sensitive detection methods are often required. Although UV absorbance offers almost universal detection ability, it suffers from relatively poor concentration sensitivity and limited selectivity. Laser-induced fluorescence (LIF) offers low detection limits but often requires analyte derivatization and more complex instrumentation. For these reasons, interest in chemiluminescence (CL) detection methods has been increasing over the past few years.

CL detection schemes [4], especially peroxyoxalates [5], have been widely applied to liquid chromatographic (LC) separations. There have been a number of CL detection schemes adapted to CE [6, 7], including luminol [8, 9], tris(2,2′-bipyridine)ruthenium(II) [10], acridinium [11], and peroxyoxalate [12–14]. An advantage of CL detectors is their simple design. They involve mixing the appropriate reagents with the CE effluent and detecting the emitted photons. While conceptually simple, mixing reagents can be difficult in CE without broadening the nanoliter volume analyte peaks because of the small volumes involved. Thus, reduced separation efficiencies have been one of the largest disadvantages of most CL detection schemes for CE.

Peroxyoxalate (PO) CL reactions are the most commonly used CL reaction in LC and have been

* *Present address*: L. L. Shultz, Department of Chemistry, University of Alberta
** *Present address*: S. Shippy, Department of Psychology, University of Ottawa
† Deceased.
Correspondence to: V. Sweedler.
Contract grant sponsors: National Institutes of Health, National Science Foundation, and Alfred P. Sloan.
Contract grant number: NS31609.

described in several reports for CE [12–14]. They involve oxidizing an aryl oxalate in the presence of a suitable fluorophore to excite the fluorophore, which then emits photons on return to the ground state. PO-CL reactions are attractive for microseparations because they exhibit high quantum efficiencies and react with a much wider range of analytes than other CL reagents. However, limited solubility in aqueous solution make the inclusion of aryl oxalates in the CE running buffer problematic. Wu and Huie overcame this problem by employing a sheathlike cell at the capillary outlet, pumping the CL reagents and the capillary effluent through the cell after a set separation time [12]. Hara et al. demonstrated PO-CL in protein separations and have improved detection by optimizing the fluorophores used for the labeling proteins [13–15]. In these examples, the separation efficiency was poor ($< 45{,}000$ theoretical plates), thereby reducing one of the advantages of CE.

Thus, one area of research in CL detection for CE has been to obtain good limits of detection (LODs) while increasing the separation efficiencies by improved methods of reagent addition. Dadoo et al. described a method based on luminol where the analytes react as they elute from the CE capillary, and the CL reaction is monitored using a parabolic mirror photomultiplier tuble (PMT) at the outlet end [9]. Zhao et al. demonstrated a sheath flow reactor with two-PMT coincidence detection that obtained 40 amol LODs with 100,000–200,000 theoretical plates for a series of isoluminol-labeled amino acids [16]. However, both methods would be difficult to adapt to the organic modifiers required of PO-CL.

Here we report an alternative method of reagent addition/mixing which allows PO-CL and other CL reactions requiring nonaqueous reagent addition and long observation times to be used with CE. The technique is based on depositing the CE effluent onto a membrane and is similar to previously described membrane deposition and detection schemes developed for radionuclide detection [17, 18]. An advantage of this deposition method is that after a separation the analytes are preserved and can be detected on the membrane using as many detection methods as necessary. Besides the radiochemical and CL methods demonstrated here, the ability to obtain matrix assisted laser desorption ionization (MALDI) mass spectra directly from membranes has been demonstrated [19]. Thus, membrane deposition offers great flexibility for CE separations in allowing

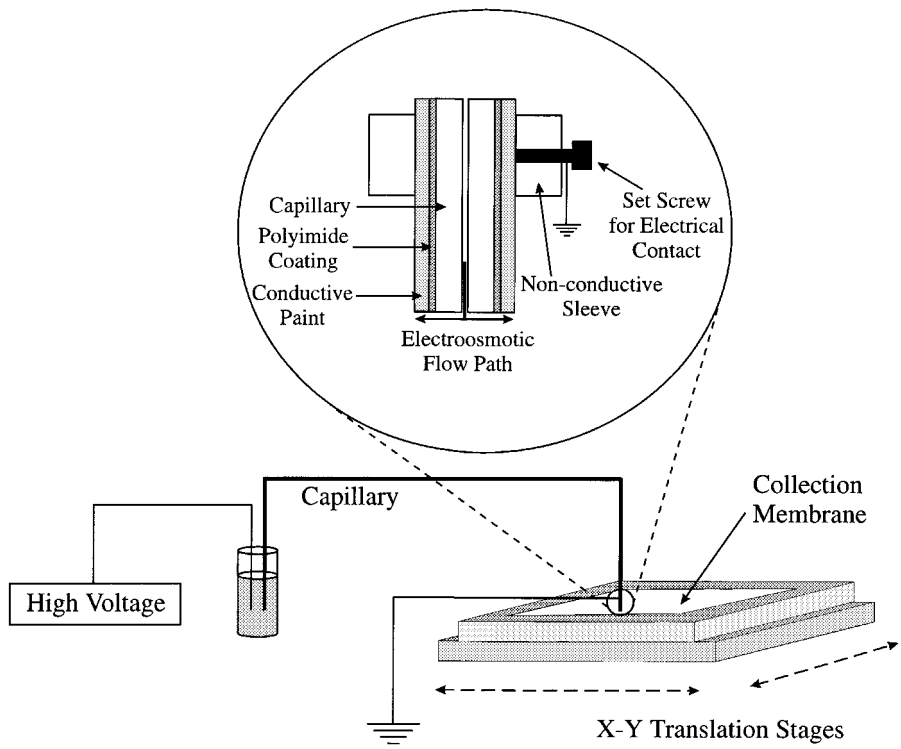

Figure 1. *Schematic of capillary electrophoresis system, showing conventional CE inlet and detail of capillary outlet from which effluent is deposited on the collection membrane.*

one to choose the appropriate detection strategy after the separation or even after other deduction modes have been used.

Integrating the emission over the majority of the CL lifetime potentially makes postcolumn methods more sensitive than capturing a transient CL signal as the reagents pass through a flow cell. Signal integration for a period exceeding the residence time of an analyte in the detector (several seconds) is generally not feasible in flowing streams. Curtis and Seitz demonstrated that the PO-CL reaction was useful for postseparation detection by using the PO-CL reaction to detect fluorophores separated by thin-layer chromatography (TLC) [20, 21]. In the original study, Curtis and Seitz used a fiber optic to transmit light emitted from the TLC plate to a PMT, measuring emission from only one spot at a time [20]. They later replaced the fiber optic and PMT with a Vidicon detector to integrate emissions from the entire TLC plate [21]. Such integrating detectors result in higher sensitivity and allow the simultaneous detection of all emitting species. Charge-coupled device (CCD) detectors [22, 23], for example, have been used to integrate CL emission in various applications, including TLC plates [22, 24], immunoassays [25–27], and biosensors [28].

In this article, analyte bands separated with CE are deposited on a membrane, and a CCD is used to integrate the CL signal arising from the PO-CL reaction. The capillary effluent is collected on a membrane that includes a peroxyoxalate CL reagent, bis(2,4,6-trichlorophenyl)oxalate (TCPO). The reaction proceeds upon application of hydrogen peroxide, and an image of the resultant CL is obtained with a CCD. Because the TCPO is present in solid form on the membrane and the hydrogen peroxide is introduced to the system as a vapor, the integrity of the deposited sample bands is maintained. The CL reaction is catalyzed by imidazole, though the presence of a catalyst is not necessary. A mixture of three dansylated amino acids is used as a model system to demonstrate separation and detection using this method. This postcolumn detection scheme allows separation parameters to be optimized independently from chemiluminescence parameters.

EXPERIMENTAL

Reagents. Dansylated lysine, valine, and glutamic acid (Dns-Lys, Dns-Val, Dns-Glu), imidazole, lithium acetate, *N*-morpholino ethane sulfonic acid (MES), and bis(2,4,6-trichlorophenyl)oxalate (TCPO) were from Sigma (St. Louis, MO). Hydrogen peroxide (30%) was from Fisher (Fair Lawn, NJ). Sodium chloride and *p*-dioxane were from EM Science (Gibbstown, NJ).

CE System. The capillary electrophoresis system (Figure 1) was similar to that used by Tracht et al. [17]. Experiments were performed using 50-μm-i.d. fused silica capillary (Polymicro, Phoenix, AZ), 60 cm in length, except when the UV absorbance detector was on-line (described below). Injections and separations were performed with 15 kV applied by a Glassman high-voltage power supply (model PS/MJ30P0400-11, Whitehouse Station, NJ). Samples (mixture of 100 μM of each Dns-Lys, Dns-Val, and Dns-Glu) were electrokinetically injected into the capillary by applying 15 kV for 1 s. A two-capillary system was used to facilitate subtraction of background chemiluminescence arising from the CE running buffer.

All capillaries were prepared by painting about 4 cm of the outlet end with Silver Print paint (GC Electronics, Rockford, IL) to provide the outlet grounding electrode. This coating was cured at 120°C for at least 2 h. The capillary tips were then sanded using Flex-I-Grit sanding film (K & S Engineering, Chicago, IL) to provide a flat, even surface to direct the electroosmotic flow outward from the inner diameter to the edge of the silver paint (Figure 1 inset). One capillary was fitted with a small section of 26-gauge Teflon tubing to provide a spacer between the capillaries to prevent the deposited lines from overlapping. The capillaries were then epoxied together and placed in a nonconductive sleeve such that the conductive screw contacts the silver paint on both capillaries. An alligator clip was used to connect the set screw to ground. This completed the CE circuit and allowed electrophoresis to occur without bulk electrolyte at the outlet.

Membrane Collection System. The capillary effluent was collected on a hydrophilic polyvinylidene fluoride (PVDF) membrane (Immobilon-CD, Millipore, Bedford, MA) which had been previously treated with a solid chemiluminescence reagent, TCPO. The TCPO was approximately 8 mM, dissolved in *p*-dioxane, and applied to the membrane via aspiration using a commercially available reagent sprayer (Kontes, Vineland, NJ). The dioxane was evaporated under a stream of nitrogen. After drying, the membrane was attached to a stage assembly consisting of perpendicular model 423 and 433 translating stages from Newport (Irvine, CA). The collection occurred by rastering the membrane across the surface of the fixed capillary tip using model 850B high-speed actuators and an MM2000 motion controller from Newport to drive the translating stages. The stage motion and the high-voltage power supply were controlled using LabView (Version 3.1.1) driving a Lab PC card (National Instruments, Austin, TX) in a Gateway 2000 P5-75 computer (North

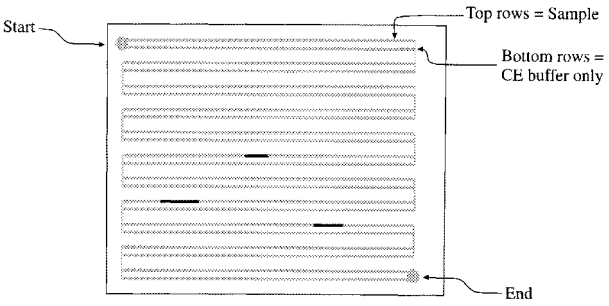

Figure 2. *Effluent pattern obtained by simultaneous deposition of two capillaries during CE. Darker regions of the drawing represent areas of greater light emission. Samples are separated in and deposited by one capillary (top rows), while the other capillary deposits only CE running buffer (bottom rows). Translating stages raster the membrane across the fixed capillary tips to create this pattern. The stages and the CE high voltage are controlled simultaneously. The high voltage is on during horizontal stage motion and off during vertical stage motion, preventing overlap of capillary effluents in the turns.*

Sioux City, SD). The high voltage was on during horizontal stage motion (x-direction) and off during vertical (y-direction) stage motion, giving the effluent pattern shown in Figure 2. The darker regions of the image represent areas of greater light emission.

Several membranes and TCPO solvents were investigated. The optimum solvent tested for TCPO was *p*-dioxane, as acetonitrile and mixed solvent systems did not completely dissolve the amount of TCPO used in these experiments. Some of the polymeric membranes dissolved upon application of *p*-dioxane. Of the membranes and other supports that did not dissolve, only the PVDF maintained the integrity of the original CE separation. Other membranes failed to wet during the CE run, so the capillary effluent was left on the membrane in large droplets. Filter papers and membranes usually absorbed the capillary effluent quickly, which resulted in broad, diffuse, sometimes overlapping deposition bands. However, the PVDF (Immobilon-CD) membrane used for these experiments produced a striated background emission (likely a result of the manufacturing process). The membrane was always arranged on the translating stage so that these striations were perpendicular to effluent deposition. The striations introduced a great deal of regularly occurring background offset, but the use of the second, reference capillary was effective in removing much of this effect.

CCD Detection System. After effluent deposition, the membrane was removed from the translating stages and placed atop a petri dish covered with a screen to hold the membrane. The dish contained the hydrogen peroxide used to initiate the CL reaction. The dish and membrane were placed below the CCD. As the hydrogen peroxide evaporated, gaseous H_2O_2 came into contact with the TCPO on the membrane, initiating the CL reaction.

The CCD and associated optics were identical to those used by Tracht and co-workers [17] and consisted of a PM512 CCD controlled by a CH260 controller (Photometrics, Tucson, AZ). The entire assembly—CCD, lenses, dish, and membrane—was completely enclosed in a light-tight box. PMIS 3.0 software (Photometrics) was used to control the CCD. In all experiments, the CCD temperature was -120°C or below, and exposure time was 15 min, unless otherwise noted.

Each PMIS image was imported into Matlab (MathWorks, Natick, MA) for processing. Spike removal routines were performed separately on the reference and sample electropherograms when appropriate. The despiking algorithm involved taking the mean and standard deviation of the three points to each side of a given point. If the value of the point was greater than the mean plus 5 times the standard deviation of the neighboring points, the point was considered a spike. The spike was then replaced with the mean of the neighboring points. The reference electropherogram was subtracted from that of the sample, and the difference plotted as CL intensity vs. elution time.

On-line UV Absorbance Detection. To provide a comparison in detection limits, a UV absorbance detector (model CV[4], Isco, Lincoln, NE) was placed about halfway between the inlet of the capillary and the membrane collection assembly. A detection window was created by burning a small area of polyimide coating off of the capillary, approximately 40 cm from the inlet end. Only the sample capillary passed through the absorbance detector. Due to the additional detector and its geometrical constraints, the capillaries were approximately 1 m in length. Thus, the voltage was increased to keep the separation times reasonable; the injections and separations were performed at 30 kV, with electrokinetic injections lasting for 1 s. A strip chart recorder was used to monitor absorbance during the CE run.

Dual Radionuclide and Chemiluminescence Detection. For this experiment, the postcolumn radionuclide detector was used as described previously [18]. Briefly, after the CE deposition, the membrane to be measured was placed on top of a phosphoimaging plate (catalog no. BAS-IIIs, Fuji, Stamford, CT) for 20 h, which created an image of radionuclide decay across the membrane. The exposed plate was read

using a phosphoimaging system (model BAS-1000, Fuji), and the plate image converted into an electropherogram. Changes from prior work included using the TCPO-treated membrane in these experiments. The CL emission was detected first, followed by radionuclide decay measurements.

The sample used was a homogenized cellular sample from the bag cell neurons of *Aplysia californica*. The sample was prepared as described previously [18] and involved incubating the abdominal ganglion in a media containing ^{35}S-Met (catalog no. SJ1015, Amersham, Arlington Heights) for 12 h so that newly synthesized met-containing peptides are labeled. After the sample was labeled, the bag cells were isolated and homogenized in a 20-μL volume. DNS-Val and DNS-Glu were added to a final concentration of 50 μM prior to use.

RESULTS AND DISCUSSION

Under ideal conditions, the CE separation process is independent of the detection process and both can be optimized separately. However, we find that many buffers produce large light emission from the membrane, most noticeably when using basic pHs. Thus, all separations reported were performed in neutral to acidic pH CE buffers. It may be possible to use basic CE buffers and then modify the membrane pH appropriately to alleviate this restriction; this will be investigated in future work.

Figure 3 shows an image of the membrane after a CE deposition. The three dansylated amino acid bands are clearly visible. Perhaps the most obvious feature of the membrane is the vertical striations. As previously mentioned, these cause baseline irregularities which greatly affect the LOD of the system. In order to reduce this effect, a two-capillary deposition method has been developed in which one of the capillaries deposits CE buffer only and the second deposits the CE sample effluent. Figure 2 schematically shows the paths of the two capillary outlets across the membrane. Unlike the previous radionuclide detection scheme [17], the high-voltage power supply is turned off during the time it takes for the capillaries to "turn" a corner in the membrane deposition process, making the two-capillary subtraction straightforward.

The rate that the membrane moves across the capillary tip is varied to determine its effect on separation efficiency. The imaging system has been optimized to view a 3 $\times$ 3-cm membrane; given this geometric constraint and the typical width of the effluent after deposition (0.35 mm), 16 passes of the sampling capillary are possible. Thus, faster capillary speeds decrease the separation time that can be collected on a single membrane. As expected, wider

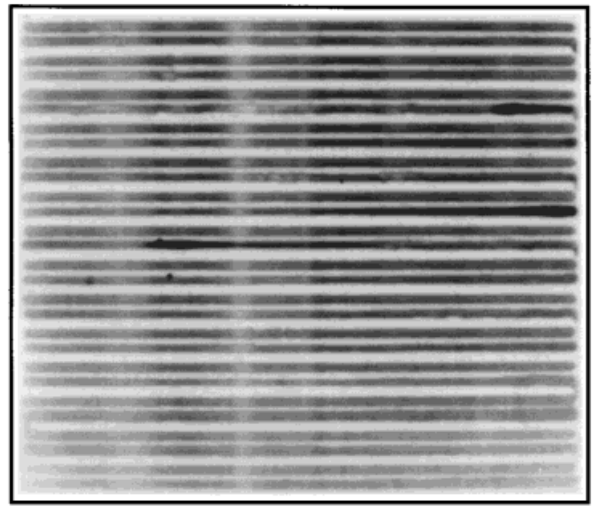

Figure 3. *CCD image of membrane after CE deposition of three separated dansyl amino acids, showing visible striations in membrane. Darker regions of the image represent areas of greater light emission. Lithium acetate CE buffer (pH 4.7); 100 μM each Dns-Lys, Dns-Val, and Dns-Glu injected electrokinetically for 1 s at 15 kV; two-capillary system employing 50 μm $\times$ 100 cm capillaries.*

sample bands are obtained when a faster collection rate is utilized, with the separation efficiency being 50,000 plates for a 0.33-mm/s movement and decreasing to 5500 plates for a 0.79-mm/s capillary movement. (Note that these separation efficiencies were obtained with no reference capillary, so they are artificially low, as discussed below.) For all experiments reported here, a 0.66-mm/s collection rate was used for all experiments to obtain narrow peaks and a 13.8-min separation time window.

Figure 4 shows representative electropherograms illustrating each step toward a final electropherogram. From the CCD image, 13 rows from the sample capillary effluent are extracted and combined end to end [Figure 4(a)], and then the blank rows from the reference capillary are similarly extracted and combined [Figure 4(b)] and the two subtracted [Figure 4(c)]. As can be seen in Figure 4(c), much of the background is removed by the subtraction of the second, reference, capillary emission. Table I quantitates the effect of the two-capillary method by showing the standard deviation of a row of the membrane under various conditions: a dark image, a membrane blank (no buffer deposited), a CE blank (where the sample capillary deposited buffer), a capillary blank (where the reference capillary deposited buffer on the same membrane), and the difference between the CE and

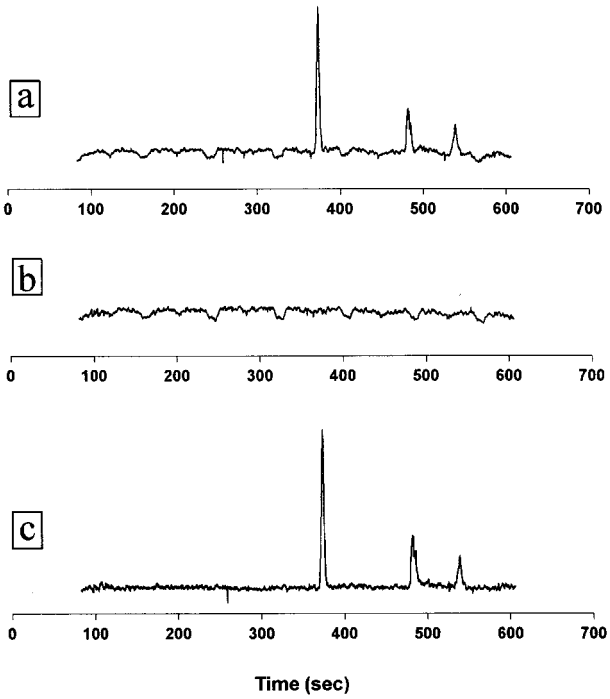

Figure 4. *Representative electropherograms extracted from sample capillary rows (a) and reference capillary rows (b), showing effects of membrane striations evident in baseline. The difference electropherogram, shown in (c), is obtained by subtracting the blank electropherogram from that of the sample and results in a smoother baseline and higher signal-to-noise ratio.*

capillary blank regions. Interestingly, the background noise increases more than an order of magnitude (from 16 to nearly 200 analog-to-digital units (ADUs)) with the presence of the buffer. The two-capillary subtraction reduces this several-fold (note that the two reads required for the subtraction should increase the read noise by 40%). However, the two-capillary subtracted result still has a standard deviation more than sixfold above the membrane background. This implies that the optimum buffer or membrane may reduce the LOD another factor of 6 by eliminating the offset and background.

Table I. *Baseline standard deviations of membrane rows.*

Membrane image extraction	σ (ADUs)
Dark image	6.73
Membrane blank, no buffer	16.04
CE sample buffer blank	192.12
CE reference buffer blank	211.72
Blank difference (sample, reference)	101.78

The separation of three dansylated amino acids (Dns-Lys, Dns-Val, and Dns-Glu) are performed in three different CE electrolytes. The three electrolytes are 30 mM NaCl/5 mM MES (pH 4.2), 30 mM imidazole–HCl (pH 7.5), and 50 mM lithium acetate (pH 4.7). The CL reactions are observed in 1-min increments. In each experiment, the membrane is placed in the CCD dark box with hydrogen peroxide, as usual, but instead of a single integration, 10 separate 1-min long integrations are taken with a 2-min delay between each exposure. Thus, the entire sequence time covers 28 min of the CL reaction. Intensities are obtained from the sequence images in Matlab by summing the same small array in each image over areas corresponding to sample bands. A similar array of emission from the CE buffer is also summed in each image. Intensities for a given peak are divided by the intensity from the buffer in the same image.

The CL emissions as a function of time are plotted in Figure 5. The NaCl/MES and lithium acetate systems both show a peak during the first 15 min of the reaction. The imidazole–HCl system appears to peak immediately upon interaction with hydrogen peroxide, because the CL reaction is already decaying by the time the sequence begins. (About 30 s lapses after initial contact between the membrane and gaseous hydrogen peroxide, while the dark box is closed and the CCD exposure is begun.) This behavior is expected because imidazole is a known catalyst of peroxyoxalate chemiluminescence reactions [29]. The remaining experiments are performed in lithum acetate buffer (pH 4.7). Although this buffer yields slightly lower CL intensities than both NaCl/MES and imidazole–HCl, it does offer some advantages. Lithium acetate gives much better membrane deposition with less arcing at the capillary tip. Lithium acetate is also preferred over imidazole–HCl, which reacts so quickly that the initial light output is difficult to record.

Figure 6 shows electropherograms obtained during the separation of dansyl valine, dansyl lysine, and dansyl glutamic acid (100 μM each). The top electropherogram [Figure 6(a)] was obtained with the on-line UV absorbance detector about 40 cm from the inlet. The periodic dips in the baseline are a result of the high voltage turning off and on during a vertical (y-direction) translation at the outlet. The bottom electropherogram [Figure 6(b)] was obtained by peroxyoxalate chemiluminescence after membrane deposition of the capillary effluent at the outlet (100 cm from the inlet). The peak shapes are similar in both methods, implying that the slight tailing observed occurs within the capillary, not as a result of effluent deposition. Absorbance gives about

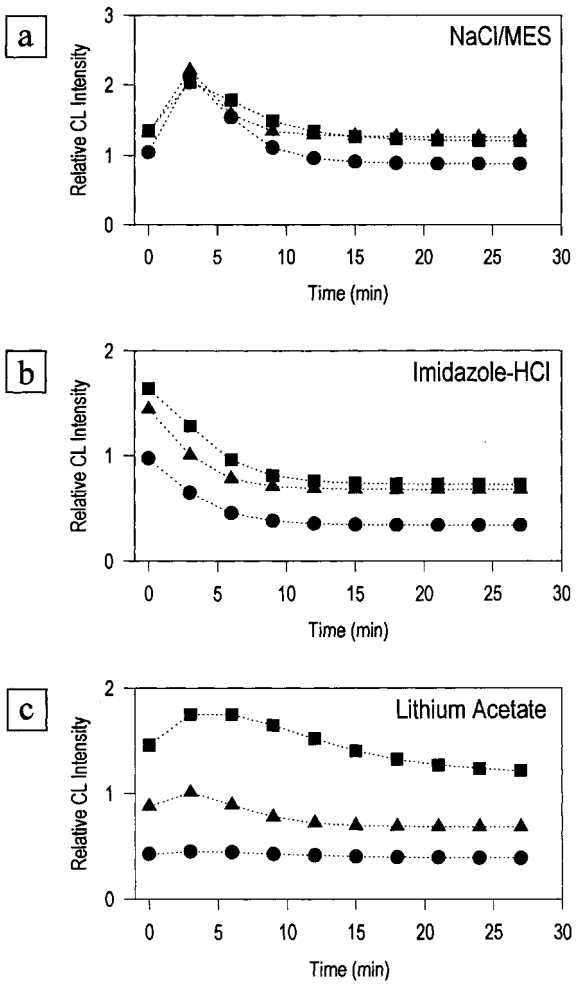

Figure 5. *Time courses for three different CE buffers used in the separation of three dansyl amino acids (● = Dns-Lys; ■ = Dns-Val; ▲ = Dns-Glu). Intensities for a given dansyl amino acid are taken relative to the intensity from the buffer in the same image.*

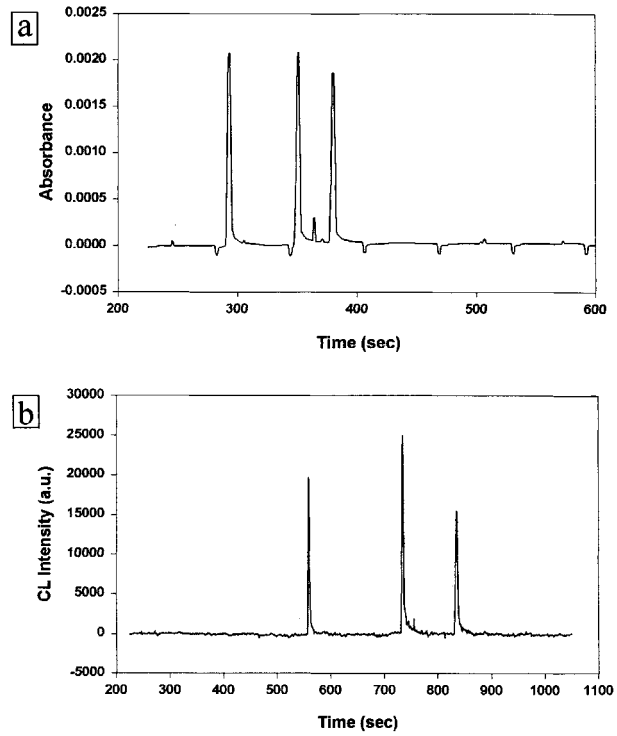

Figure 6. *Electropherograms obtained during the separation of 100 μM each Dns-Lys, Dns-Val, and Dns-Glu, (a) using an on-line absorbance detector about 40 cm from the inlet (λ = 254 nm) and (b) performing membrane collection at the outlet simultaneously. Lithium acetate CE buffer (pH 4.7); 100 μM each Dns-Lys, Dns-Val, and Dns-Glu injected electrokinetically for 1 s at 15 kV; two-capillary system employing 50 μm × 100 cm capillaries. Periodic dips in the baseline in (a) are a result of the CE high voltage turning off and on during a "turn" at the outlet.*

68,000 plates for Dns-Glu, and the peroxyoxalate CL method gives about 170,000 plates. The 3σ detection limit for Dns-Glu is 1 μM (8.7 fmol) for absorbance and about 1.5 μM (13 fmol) for this peroxyoxalate CL method. Although the conditions for this separation are not fully optimized, this shows that the two methods are comparable. Wu and Huie [12] obtained LODs of ~ 100 mM (1.0 fmol) for dansyl amino acids with separation efficiencies of about 10,500 plates. Although they obtained about an order of magnitude better LODs due to their lower CL background, the pressure-driven elution of their separated sample resulted in about an order-of-magnitude poorer separation efficiencies. The membrane collection method has a fairly narrow working range: the upper limit, where the CCD reaches full-well capacity, is between 300 and 500 μM, depending upon the particular dansylated amino acid. However, due to the membrane striations and inhomogeneous surface chemistry, the method does not yield a reproducible working curve. Compared to previous (TLC, for example) area-based PO-CL detection methods, the mass detection limits are about 900 times better [20].

One of the largest advantages of the postcolumn membrane deposition is that multiple detection modalities can be used as needed after a separation. Radiochemical detection offers extremely low detection limits and the ability to selectively label amino acids and peptides using cellular machinery. Radionuclide detection is very selective; for example, by culturing cells in media containing radiolabeled precursors, only newly synthesized compounds using the radiolabel can be detected. However, obtaining internal standards for radionuclide detection can be

difficult, and so we have investigated adding CL active compounds to the CE/radionuclide separations and then using both CL and radionuclide detection. By combining these detection schemes, nonradiolabeled standards can be incorporated and the standards and radionuclides can be measured separately using the two detection modes, with Figure 7 showing preliminary results demonstrating this combination. Specifically, the separation of two dansylated amino acids (detectable by CL) spiked into ^{35}S methionine-labeled cellular homogenate (detectable by radionuclide detection) is shown. Figure 7(b) shows the entire electropherogram using CL detection with only a single capillary pass from the radionuclide detection shown in Figure 7(a). Based on previous calibration results, the peak labeled with ^{35}S-methionine contains approximately 10 amol of radiolabel. While further improvements are needed to allow precise electropherogram registration between detection modes, this result demonstrates the ability to combine various membrane detection schemes from a single electropherogram.

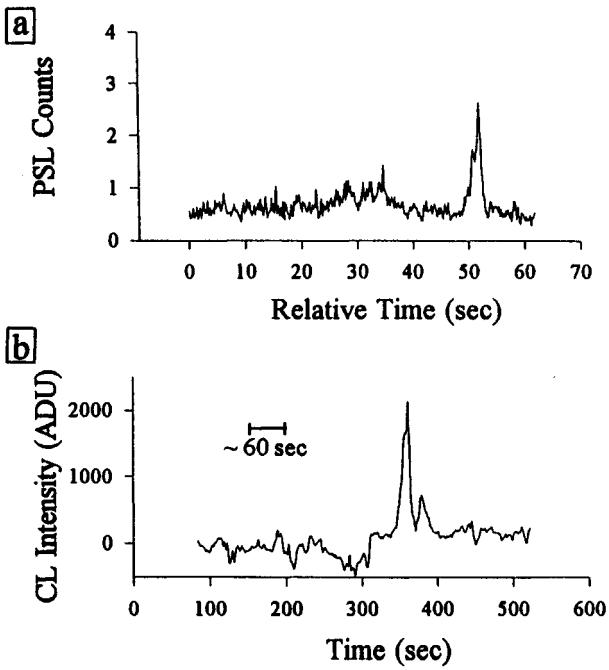

Figure 7. *A single electropherogram detected with postcolumn CL detection and radionuclide detection. Specifically, 50 μM each Dns-Val and Dns-Glu were spiked into a radiolabeled A. californica bag cell homogenate. (a) A single 60 s trace of the membrane using radionuclide detection with the major peak being an unidentified cellular component at about the 10-amol level. (b) CL detection showing the DNS-labeled components.*

CONCLUSIONS

A postcolumn membrane collection system has been developed that obtains high separation efficiency and preserves the separated sample for later detection. While the separation and detection of dansylated amino acids have been demonstrated, the PO-CL chemistry is well suited for many additional classes of analytes. Most intriguing are those analytes that are natively fluorescent such as bilirubins [30] and peptides or proteins containing the amino acids phenylalanine, tyrosine, and tryptophan and the neurotransmitters derived from them, such as serotonin and dopamine. Although such species can be detected by UV LIF detection, the high cost of UV lasers often makes this impractical. As the CCD currently used in this detection system is insensitive in the UV, the current system cannot be used to examine peptides without derivatization. The use of the appropriate CCDs and optics would alleviate this restriction and should provide for moderate sensitivity for such analytes without requiring an ultraviolet laser.

We expect membrane CL methods to be used in conjunction with other compatible detection methods, as demonstrated with radiochemistry, to obtain complimentary data and to confirm results. MALDI-TOF (time-of-flight) mass spectrometry allows the detection and characterization of peptides, and this detection method should be compatible with the other CE/membrane detectors and is currently under investigation. Also, with careful manipulation of reagents, multiple CL chemistries may be combined on one membrane for a single CE separation for greater selectivity. Lastly, the use of postcolumn membrane detection allows samples to be recovered for additional biochemical assays as needed.

ACKNOWLEDGMENTS

The authors dedicate this manuscript to Timothy Nieman, a wonderful colleague, mentor, and friend. We also acknowledge Kurt Oldenburg for assistance with programming and Scott Tracht for help with initial system development.

REFERENCES

1. N.A. Guzman, Ed., *Capillary Electrophoresis Technology*. Vol. 64 (Dekker, New York, 1993).
2. J.P. Landers, Ed., *Handbook of Capillary Electrophoresis* (CRC Press, Boca Raton, FL, 1993).
3. R. Kuhn and S. Hofstetter-Kuhn, *Capillary Electrophoresis*: *Principles and Practice* (Springer-Verlag, Berlin, 1993).
4. K. Imai, A. Nishitani, H. Akitomo, and Y. Tsukamoto, *J. Biolumin. Chemilumin.* **4,** 500 (1989).
5. P.J.M. Kwakman and U.A.Th. Brinkman, *Anal. Chim. Acta* **266,** 175 (1992).

6. W.R.G. Baeyans, B.L. Ling, K. Imai, A.C. Calokerinos, and S.G. Schulman, *J. Micro. Sep.* **6,** 195 (1994).
7. A.M.G. Campana, W.R.G. Baeyens, and Y. Zhao, *Anal. Chem.* **69,** 83A (1997).
8. R. Dadoo, A.G. Seto, L.A. Colon, and R.N. Zare, *Anal. Chem.* **66,** 303 (1994).
9. R. Dadoo, L.A. Colon, and R.N. Zare, *J. High Resolut. Chromatogr.* **15,** 133 (1992).
10. G.A. Forbes, T.A. Nieman, and J.V. Sweedler, *Anal. Chim. Acta* **347**, 289 (1997).
11. M.A. Ruberto and M.L. Grayeski, *J. Micro. Sep.* **6,** 545 (1994).
12. N. Wu and C.W. Huie, *J. Chromatogr.* **634,** 309 (1993).
13. T. Hara, J. Yokogi, S. Okamura, S. Kato, and R. Nakajima, *J. Chromatogr. A* **652,** 361 (1993).
14. T. Hara, S. Kayama, H. Nishida, and R. Nakajima, *Anal. Sci.* **10,** 223 (1994).
15. K. Tsukagoshi, A. Tanaka, R. Nakajima, and T. Hara, *Anal. Sci.* **12,** 525 (1996).
16. J.Y. Zhao, J. Labbe, and N.J. Dovichi, *J. Micro. Sep.* **5,** 331 (1993).
17. S. E. Tracht, V. Toma, and J.V. Sweedler, *Anal. Chem.* **66,** 2382 (1994).
18. S.E. Tracht, L. Cruz, C.M. Stobba-Wiley, and J.V. Sweedler, *Anal. Chem.* **68,** 3922 (1996).
19. H.Y. Zhang and R.M. Caprioli, *J. Mass Spectrom.* **31,** 1039 (1996).
20. T.G. Curtis and W.R. Seitz, *J. Chromatogr.* **134,** 343 (1977).
21. T.G. Curtis and W.R. Seitz, *J. Chromatogr.* **134,** 513 (1977).
22. Q.S. Hanley, C.W. Earle, F.M. Pennebaker, S.P. Madden, and M.B. Denton, *Anal. Chem.* **68,** 661A (1996).
23. J.V. Sweedler, *Crit. Rev. Anal. Chem.* **24,** 59 (1993).
24. Y. Liang, M.E. Baker, B.T. Yeager, and M.B. Denton, *Anal. Chem.* **68,** 3885 (1996).
25. C.S. Martin and I. Bronstein, *J. Biolumin. Chemilumin.* **9,** 145 (1994).
26. R.K. Kobos, B.A. Blue, C.W. Robertson, and L.A. Kielhorn, *Anal. Biochem.* **224,** 128 (1995).
27. P. Lorimier, L. Lamarcq, A. Negoescu, C. Robert, F. Labatmoleur, F. Graschappuis, I. Durrant, and E. Brambilla, *J. Histochem. Cytochem.* **44,** 665 (1996).
28. H.H. Gao, Z.P. Chen, J. Kumar, K.K. Tripathy, and D.L. Kaplan, *Opt. Eng.* **34,** 3465 (1995).
29. N. Hanaoka, R.S. Givens, R.L. Schowen, and T. Kuwana, *Anal. Chem.* **60,** 2193 (1988).
30. L.P. Palilis, A.C. Calokerinos, and N. Grekas, *Anal. Chim. Acta* **333,** 267 (1996).